Physical pathways and utilization of nitrate supply to the giant kelp, *Macrocystis pyrifera*

Jonathan P. Fram[1] *and Hannah L. Stewart*[2]
Marine Science Institute, University of California at Santa Barbara, Santa Barbara, California 93106

Mark A. Brzezinski
Marine Science Institute, University of California at Santa Barbara, Santa Barbara, California 93106; Department of
Ecology Evolution and Marine Biology, University of California at Santa Barbara, Santa Barbara, California 93106

Brian Gaylord
Bodega Marine Laboratory and Section of Evolution and Ecology, University of California at Davis, Bodega Bay,
California 94923

Daniel C. Reed
Marine Science Institute, University of California at Santa Barbara, Santa Barbara, California 93106

Susan L. Williams
Bodega Marine Laboratory and Section of Evolution and Ecology, University of California at Davis, Bodega Bay,
California 94923

Sally MacIntyre
Marine Science Institute, University of California at Santa Barbara, Santa Barbara, California 93106; Department of
Ecology Evolution and Marine Biology, University of California at Santa Barbara, Santa Barbara, California 93106

Abstract

To determine the relative importance of different sources of nitrate to the annual nitrogen needs of the giant kelp *Macrocystis pyrifera,* we measured ambient nitrate concentrations at a kelp forest for 13 months and characterized nitrate delivery using water column thermal structure and flow data collected in the forest and at its offshore edge. The forest's monthly nitrate supply varied by a factor of 50, while measured net nitrogen acquisition varied only fivefold. Maximum net nitrogen acquisition rates for fronds in the forest interior were 0.18 mmol N g^{-1} month^{-1} during spring upwelling in 2005 and declined fourfold during autumn until upwelling resumed the following year. Modeled gross nitrogen uptake with consideration of Michaelis–Menten kinetics for nitrate and mass transfer limitation was higher than observed net acquisition except during the warm stratified summer and autumn months, when net acquisition exceeded modeled gross uptake. This shortfall indicates that the kelp forest received over half its nitrogen from sources other than nitrate such as ammonium from epibionts. Most of the nitrate in the forest was delivered as a result of upwelling-favorable winds and convection. Internal waves and local streams contributed <9% of the nitrate delivered to the forest on an annual basis and 20% during stratified periods. Kelp used less than 5% of the nitrate supplied to the forest. Nitrate delivery to this modest sized kelp forest was roughly equivalent between alongshore (45%) and cross-shore flows (55%), which distinguishes it from large kelp forests in which cross-shore flows dominate exchange.

[1] Corresponding author (jfram@msi.ucsb.edu).
[2] Present address: Friday Harbor Labs, University of Washington, Friday Harbor, Washington 98250.

Dense forests of the giant kelp *Macrocystis pyrifera* support some of the highest rates of primary productivity of any ecosystem on Earth (Mann 1973). Elongation rates of individual fronds of *M. pyrifera* can exceed 50 cm d^{-1}, making it one of the fastest growing autotrophs in the world (Clendenning 1971). Such high growth creates a demand for nutrients that may exceed supply during periods when the water column becomes stratified and upwelling of nutrients into nearshore areas relaxes (Gerard 1982*b*; Zimmerman and Kremer 1986). The balance between the demand for and the supply of nutrients to giant kelp forests has been shown to be important in determining its growth and survival (Graham et al. 2007).

Nitrogen is the nutrient believed to most frequently limit *Macrocystis* growth off the coast of southern California (Jackson 1977; Wheeler and North 1981), and most studies of kelp nutrient requirements have focused on nitrate's role in determining giant kelp growth and survival. Rates of nitrate uptake in giant kelp decline dramatically at ambient concentrations of less than 1 μmol L^{-1} (Gerard 1982*b*; Zimmerman and Kremer 1984), and growth becomes nitrogen limited if nitrate concentrations remain low for more than about 3 weeks. The importance of nitrogen as a potentially limiting resource follows seasonal patterns in the Southern California Bight. Nitrate is relatively abundant during winter when deepening of the mixed layer entrains nitrate into surface waters and during brief periods of spring upwelling when concentrations reach their annual maximum. In contrast, nitrate concentrations in surface waters decline during summer and most of autumn. During the latter periods, other supply mechanisms, such as internal waves, can be important for sustaining kelp growth (Gerard 1982*b*; Jackson 1984; Zimmerman and Kremer 1984). McPhee-Shaw et al. (2007) provide the first budget of nutrient supply to the inner shelf pertinent to kelp forests. Their 2 yr study showed that upwelling supplies more than 70% of the nitrate to the inner shelf and internal waves in summer provide 9–12%. Terrestrial loading varies annually and supplies between 4% and 35% of the nitrate. Owing to different intensities of upwelling along the coast, ambient concentrations just offshore of different kelp forests varied spatially at scales of 20 km. Regenerated sources of inorganic nitrogen in the form of ammonium released by epibionts have also been identified as a potential nitrogen source for kelp in summer (Gerard 1982*b*; Hepburn and Hurd 2005). Despite these efforts to address supply, kelp utilization of these various sources has not been quantified.

The supply of nitrate to giant kelp also depends on currents (both along and across shore), waves, and modification of these flows by the presence of the kelp forest. Flow speeds inside a kelp forest attenuate relative to those outside due to drag (Jackson 1977, 1984, 1998). For example, the fraction of alongshore flow penetrating a moderate-sized kelp forest (hundreds of meters) can be reduced by nearly half as kelp density increases seasonally in summer (Gaylord et al. 2007). Within the forest, nitrate supply is a function of water flow characteristics, the degree of vertical stratification of the water column, and levels of nitrate depletion by upstream kelp (Jackson 1977).

Knowledge of the various mechanisms that deliver nitrogen to kelp forests and the ability of kelp to exploit them are needed to fully understand the potential for nitrogen to limit the growth of giant kelp. Developing such a budget further requires understanding the processes that regulate the flux of nitrate into the kelp blade. That is, the fraction of nitrate delivered to a kelp frond that is taken up to support growth depends upon the physical mass transport of nitrate to its surface (Stevens et al. 2003) and the physiological transport of nitrate across the cell wall (Gerard 1982*b*). Previous studies arrived at contrasting views regarding the relative importance of these two processes. Laboratory studies have shown that rates of nitrate uptake in *M. pyrifera* were not mass transfer-limited at steady flow speeds greater than 4 to 6 cm s^{-1} (Wheeler 1980; Gerard 1982*c*; Hurd et al. 1996), and Gerard (1982*b*) concluded that mass-transport limitation in giant kelp is uncommon because such low flows are atypical of field conditions due to wave exposure. In contrast, a modeling study that incorporated the effects of both oscillatory and steady currents on nitrogen uptake concluded that significant mass transfer limitation of nitrogen uptake occurs in the morphologically similar congener *Macrocystis integrifolia* (Stevens et al. 2003).

In the following, we present the first comprehensive study of nitrogen supply to and acquisition by an entire kelp forest. We quantify the role of large- and small-scale physical processes, kelp bed morphometry, and biological processes. To describe the spatial and temporal variation in nitrogen supply and acquisition, we combined a 13-month time series of observations of the thermal structure and current velocities inside and outside of a giant kelp forest with measurements of seawater nitrate concentrations, the distribution of kelp biomass within the forest, and nitrogen acquisition rates measured by two independent methods. We modeled nitrogen supply and acquisition to kelp in the forest using these data taking into account mass transfer and nitrogen uptake kinetics. We compared measured values of nitrate supply to modeled values of nitrogen acquisition and thus quantified not only the fraction of nitrate delivered to the kelp forest by various physical processes but also the percentage utilized. Discrepancies between measured nitrogen uptake and modeled acquisition of nitrate allowed us to show when biological processes such as recycling made an important contribution to supply.

Methods

Field site—Field measurements were collected at Mohawk Reef (34°23′38.7″N, 119°43′44.8″W) located off the coast of Santa Barbara, California (Fig. 1). *M. pyrifera* at this site grows at depths of 5 to 9 m atop a rocky outcrop whose dimensions are approximately 300 m alongshore and 180 m cross shore (Gaylord et al. 2007).

Water column properties and hydrodynamics—Measurements of velocity and temperature were collected from 21 March 2005 to 01 May 2006 at two stations, one in the interior of the kelp forest at 8.0-m depth, 190 m from shore (hereafter inside station), and one offshore the kelp forest at 10.4-m depth, 300 m from shore (hereafter outside
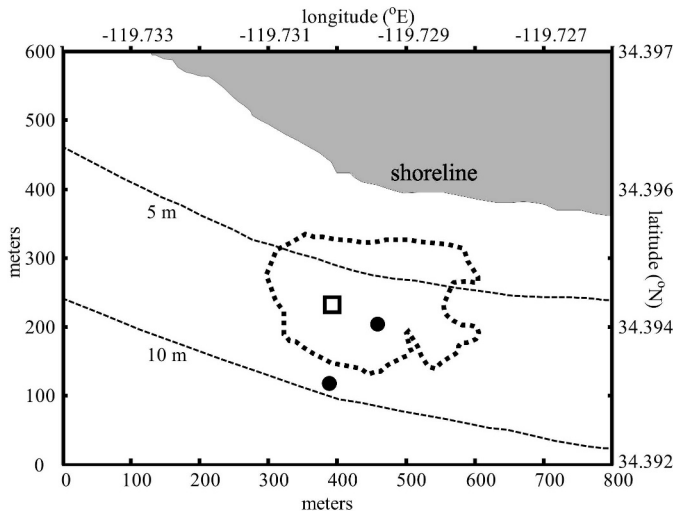
Fig. 1. Bathymetric map of Mohawk Reef site showing the coverage (dotted outline) of *M. pyrifera* in September 2005. The inside and outside stations are marked by closed circles and the open square is the location of SBCLTER monthly biomass measurements.

station). Water velocity was measured at the inside station with a bottom-mounted upward-looking 1,200-kHz acoustic Doppler current profiler (ADCP; Teledyne RD Instruments (RDI)) and at the outside station with a bottom-mounted upward-looking 600-kHz ADCP. The ADCPs collected a 1- to 4-min burst of 1 Hz velocity data every 2 to 8 min at 0.5-m depth intervals from 1.3 m above the bottom to 0.8 m below the water surface. Thermal structure, used to characterize movement of water masses within the kelp forest, was determined via temperature measurements acquired every 10 s using thermistors (Richard Brancker Research TR-1050, 0.002°C accuracy) spaced 1-m apart (from 0.6 m above the seafloor to just above mean sea level) on polyvinyl chloride spar buoys placed at the inside and outside stations. Seawater density was calculated from the equation of state for seawater using temperature at Mohawk Reef and depth-averaged salinity data from a mooring at Stearns Wharf, which is located 5 km east of Mohawk Reef. To determine density stratification, we calculated depth-averaged buoyancy frequency, $N = \sqrt{-g/\rho(d\rho/dz)}$, where g is gravity, ρ is density, and z is depth. Water motions from waves were incorporated into our estimates of flow using wave data extracted from National Oceanic and Atmospheric Association (NOAA) buoy 46216 (www.ndbc.noaa.gov), located 9 km southwest of Mohawk Reef. We confirmed that the dominant wave period and significant wave height measurements from the NOAA buoy were nearly equivalent to those at Mohawk Reef by comparing data from an 18-d deployment of two RDI 600-kHz wave-measuring ADCPs 80 m west of the inside station during January and February 2006 (data not shown).

Water column nitrate concentration—Nitrate concentration was measured in situ at Mohawk Reef throughout the study using a nitrate autoanalyzing sensor (EnviroTech, Models NAS-2E and NAS-3X) moored 4 m above the

bottom 10.5 m southwest of the outside ADCP. To validate the modeled relationship between nitrate concentrations inside and outside the forest, an additional nitrate autosensor (NAS) was deployed adjacent to the inside thermistor chain for 2 weeks in fall 2006 at the same depth.

We reconstructed nitrate concentration at all depths at both the inside and outside stations using temperature–nitrate correlations. From the NAS and its associated temperature data, we modeled nitrate concentration as a function of temperature with an exponential

$$C = k_1 e^{-k_2 T} \quad (1)$$

where C is nitrate concentration (μmol L^{-1}), k_1 is 2.8×10^4 (μmol L^{-1}), k_2 is 0.64 (1°C), and T is temperature. This relationship ($r^2 = 0.87$) is consistent with results from previous studies of this region (Jackson 1977; Zimmerman and Robertson 1985; McPhee-Shaw et al. 2007).

We further refined the nitrate concentration–temperature relationship to account for eddies that move past Mohawk Reef that have varying nutrient concentration to temperature relationships (Beckenbach and Washburn 2004; McPhee-Shaw et al. 2007). An additional scaling factor was defined using the temperature at the NAS and the temperature at the location being modeled. For each modeled time step, we accounted for the change in the concentration to temperature relationship over time by offsetting our concentration estimates from Eq. 1 by the measured NAS concentration minus the concentration estimated from the temperature measured by a thermistor on the NAS ($C_{NAS} - C_{NAS}^{est}$), where $C_{NAS}^{est} = k_1 e^{-k_2 T_{NAS}}$. Because concentration also changes more at low than at high temperatures, this offset was weighted by the ratio of concentration at depth z from Eq. 1 to the concentration estimated from the NAS temperature ($C_z / C_{NAS}^{est} = e^{-k_2(T_z - T_{NAS})}$). Together,

$$C_z^{est} = k_1 e^{-k_2 T_z} + \left(C_{NAS} - k_1 e^{-k_2 T_{NAS}}\right) e^{-k_2(T_z - T_{NAS})} \quad (2)$$

which improved our estimates over Eq. 1 by 35% ($0.35 = \overline{\left(\left|C_z^{est} - k_1 e^{-k_2 T_z}\right|/k_1 e^{-k_2 T_z}\right)}$).

Measurements of net nitrogen uptake by kelp—Rates of net nitrogen uptake by kelp at Mohawk Reef were calculated using two methods: one method focused on the net uptake by the entire forest, and the other examined uptake by a select subset of fronds to isolate vertical and cross-shore differences in nitrogen acquisition. Together these methods allowed us to assess how seasonal and spatial changes in giant kelp biomass and nitrate concentration affected nitrogen uptake and the ability of nitrate to meet the kelp's nitrogen demand.

Net nitrogen uptake by the kelp forest at Mohawk Reef was estimated in a 40 m × 40 m section of the forest monthly and computed seasonally by the Santa Barbara coastal long-term ecological research project (hereafter SBCLTER; Rassweiler et al. in press). Briefly, allometric relationships involving kelp length and mass were combined with monthly field measurements of kelp abundance, size, nitrogen content, and rates of frond and whole plant loss to calculate the average mass of new kelp nitrogen

produced per existing kelp nitrogen mass per day, which was then averaged over each season.

Spatial patterns of net nitrogen uptake on select fronds both inside the forest and at its seaward edge were determined from changes in frond size and the tissue nitrogen content of mature blades on actively growing fronds that reached the water surface. Because losses of dissolved nitrogen compounds were not measured, the calculated rates represent net uptake and thus are a minimum estimate of kelp nitrogen demand. Elongation rates were determined by measuring the length of individual growing canopy fronds at the beginning and end of seven periods, each spanning 8 to 14 d, from March 2005 to April 2006. During each sampling period measurements of frond length and mass, blade area and nitrogen content, and number of blades per frond, in the water column and the surface canopy were taken on 10 to 20 fronds at the outside edge and interior of the kelp forest. We estimated stipe nitrogen content as 55% of the blade nitrogen content (Rassweiler, Arkema, and Reed, unpubl. data). These data were used to calculate net nitrogen uptake per frond as

$$\frac{\text{net N uptake}}{\text{frond}}$$

$$= \frac{d}{dt} \left(\sum_{j=1}^{2} \sum_{i=1}^{2} \left(\frac{\text{wet mass}}{\text{length}} \frac{\text{mol N}}{\text{wet mass}} \frac{\text{length}}{\text{frond part}} \right)_{ij} \right) \quad (3)$$

where i is the index for the water column ($i = 1$) and canopy ($i = 2$) part of each frond and j is the index for the blade ($j = 1$) and stipe ($j = 2$) portions of each frond part. This quantity is net rather than gross uptake because it does not account for dissolved nitrogen losses from the kelp to the ocean or for grazing losses that do not break or completely remove fronds. By only sampling fronds that maintained their apical meristems for the 8 to 14 measurement periods, we measured uptake, as opposed to measuring the rate change of nitrogen content in canopy fronds. The derivative in Eq. 3 yields a term corresponding to the nitrogen in new growth plus terms reflecting the change in tissue nitrogen content and the change in tissue mass per length of the frond.

$$\frac{\text{net N uptake}}{\text{frond}} = \sum_{j} \sum_{i} \left(\begin{array}{c} \frac{\text{wet mass}}{\text{length}} \frac{\text{mol N}}{\text{wet mass}} \frac{\partial}{\partial t} \left(\frac{\text{length}}{\text{frond part}} \right) \\ + \frac{\text{wet mass}}{\text{length}} \frac{\partial}{\partial t} \left(\frac{\text{mol N}}{\text{wet mass}} \right) \frac{\text{length}}{\text{frond part}} \\ + \frac{\partial}{\partial t} \left(\frac{\text{wet mass}}{\text{length}} \right) \frac{\text{mol N}}{\text{wet mass}} \frac{\text{length}}{\text{frond part}} \end{array} \right)_{ij} \quad (4)$$

Dividing by mass per frond yields the net molar acquisition rate of nitrogen per wet mass of kelp.

$$\text{net uptake}_{\text{measured}} =$$

$$\sum_{j} \sum_{i} \left(\begin{array}{c} \frac{\text{mol N}}{\text{wet mass}} \frac{\partial}{\partial t} \left(\frac{\text{length}}{\text{frond part}} \right) \frac{\text{frond part}}{\text{length}} \\ + \frac{\partial}{\partial t} \left(\frac{\text{mol N}}{\text{wet mass}} \right) + \frac{\text{mol N}}{\text{wet mass}} \frac{\partial}{\partial t} \left(\frac{\text{wet mass}}{\text{length}} \right) \frac{\text{length}}{\text{wet mass}} \end{array} \right)_{ij} \quad (5)$$

Rates of net nitrogen uptake were determined for the

interior of the forest near the inside station and for the offshore edge of the forest between the inside and outside stations.

Modeled nitrate uptake—Gross rates of nitrate uptake were modeled by considering physiological transport kinetics, mass transfer across the diffusive kelp boundary layer due to waves and currents, and ambient nitrate concentrations. The model incorporated morphological characteristics of kelp that defined the blade area per kelp mass and thus uptake per mass.

We modeled physiological constraints on gross nitrate uptake with the Michaelis–Menten function and parameters determined by Gerard (1982*b*) and Kopczak (1994)

$$R = V_{\max} \frac{C_0}{K_m + C_0} \quad (6)$$

where the uptake rate (R, μmol area^{-1} time^{-1}) relates to the nitrate concentration immediately at the blade surface (C_0) and the half-saturation constant (K_m), which is the nitrate concentration where uptake is 50% of the maximum rate ($V_{\max}$). Gerard (1982*b*) gives upper and lower bounds of these parameters for nitrate flux to *M. pyrifera* (K_m and $V_{\max}$ are 14.5 μmol N L^{-1} and 2.7 μmol N L^{-1} (wet g)$^{-1}$ h^{-1} or 4.3 μmol N L^{-1} and 1.7 μmol N L^{-1} (wet g)$^{-1}$ h^{-1}). For the purposes of this study, we computed results using both sets of Gerard's parameters and averaged them, since values of monthly low-pass filtered R simulated using the two sets of parameters differed by less than 15%. The mass-specific values of $V_{\max}$ reported by Gerard were converted to surface area specific rates because nitrate transport occurs across the membranes of cells with little or no contribution from interior structures (Miflin 1974; Kamachi et al. 1987). In addition, we invoked a light dependence for $V_{\max}$ based on Gerard (1982*b*) with nighttime values being one half of maximum daytime values. $V_{\max}$ was also assumed to decline with the lower light levels at depth assuming exponential decay of $V_{\max}$ that yielded 55% of surface $V_{\max}$ at 12-m depth. $V_{\max}$ changes due to the nutrient history of the kelp were also taken into account. Kopczak's $V_{\max}$ for nutrient-replete kelp was 34% smaller than for nitrogen-starved kelp. Gerard's field conditions were intermediate between nitrogen-starved and nitrogen-replete conditions; therefore we augmented $V_{\max}$ by 17% during nutrient-starved portions of model runs, and we reduced $V_{\max}$ by 17% during nutrient-replete conditions.

Nitrate uptake reduces nitrate concentration at the blade surface (C_0), necessitating its replenishment in the blade boundary layer via mass-transport processes, which we model as

$$F = \beta(C_\infty - C_0) \quad (7)$$

where F is the flux to the blade surface (μmol area^{-1} time^{-1}), β is the mass transfer velocity (m s^{-1}), and C_∞ is the ambient nitrate concentration far from the blade. The flux, F, equals the uptake rate (R) at steady state. We used a recent formulation for β that describes a "boundary layer stripping" capacity for surface gravity waves (Stevens et al. 2003). In this model, nitrogen flux to the blade surface is the sum of

uptake from currents (J_u) and waves (J_w). For currents:

$$J_u = \frac{DC_\infty}{\delta_D} \qquad (8)$$

D, the molecular diffusivity of nitrate, can be approximated as a linear function of temperature for this application (Li and Gregory 1974):

$$D = T_{\text{Celsius}} 3.65 \times 10^{-11} + 9.72 \times 10^{-10} \, (\text{m}^2 \, \text{s}^{-1}) \qquad (9)$$

Diffusion boundary layer thickness, δ_D, is modeled as an empirical function of current speed (Stevens and Hurd 1997). J_w depends on δ_D, the dominant wave period (T_{wave}), and C_∞

$$J_w = \frac{4C_\infty \delta_D}{T_{\text{wave}}} \sum_{n=1}^{\infty} \left(\frac{1 - \exp\left(-\frac{Dn^2\pi^2 T_{\text{wave}}}{2\delta_D^2}\right)}{n^2\pi^2} \right) \qquad (10)$$

According to this model, an eddy that forms twice each wave period completely strips away the nitrate-depleted diffusion boundary layer and replaces it with ambient water.

To evaluate whether uptake is limited by kinetic constraints or mass transport, we followed Sanford and Crawford (2000) to compute R in molar flux units of (μmol NO$_3$/m^2 s) as a function of these two processes:

$$R = \frac{V_{\max}C_\infty}{K_m\left(\frac{C_\infty}{K_m} + \frac{1}{2}\left(\gamma + \sqrt{\gamma^2 + 4\frac{C_\infty}{K_m}}\right)\right)} \qquad (11)$$

where $\gamma = 1 + (V_{\max}/\beta K_m) - (C_\infty/K_m)$. The model was run with an hourly time step. For presentation, results were subjected to a 30-d low-pass filter to show changes over the time scales that kelp growth and internal nitrogen stores respond to changes in ambient nitrate (Gerard 1982*a,b*; Zimmerman and Kremer 1986). To more efficiently compare the degree to which nitrate flux is limited by mass transfer versus kinetics, results were also expressed in terms of a dimensionless mass transfer coefficient, $\beta K_m : V_{\max}$, and a dimensionless uptake rate, $RK_m/C_\infty V_{\max}$ (Sanford and Crawford 2000). The dimensionless mass transfer coefficient is the ratio of the mass transfer coefficient β to the initial slope of the Michaelis–Menten function ($\alpha = V_{\max} : K_m$). Higher values of $\beta : \alpha$ indicate reduced control of nitrate flux by mass transport. Similarly, the dimensionless uptake rate, $RK_m/C_\infty V_{\max}$, is the ratio of the actual nitrate flux to the maximum possible nitrate flux dictated by kinetics, so that increases in $RK_m/C_\infty V_{\max}$ indicate greater control of overall nitrate flux by the combination of kinetics and mass transport.

With this model, the uptake per frond wet mass was computed as the flux of nitrogen times the surface area per mass:

$$\text{gross uptake}_{\text{modeled}} = R\left(\frac{\text{blades}}{\text{length}}\frac{\text{area}}{\text{blade size}}\frac{2 \text{ sides}}{\text{blade}}\right.$$
$$\left. + \pi \text{ stipe diameter}\right)\frac{\text{frond length}}{\text{wet mass}} \qquad (12)$$

where R is the nitrate flux as described above. We addressed the differences in uptake associated with differences in surface area per mass along fronds by computing uptake separately in the canopy and at the top, middle, and bottom thirds of the noncanopy portion of the water column, where the bottom included the holdfast, sporophylls, and the bottom of each frond. Modeled gross uptake for fronds in the 40 m × 40 m SBCLTER study area was computed by the same methods. The SBCLTER area results rely on allometric relationships measured for 60 plants from this and adjacent kelp forests measured concurrently with our 13-month study (Gaylord unpubl.). We refer to gross uptake rather than just uptake to emphasize that our uptake model does not account for dissolved losses.

Nitrate availability and utilization—We examined the nitrate supply to Mohawk Reef from upwelling, internal waves, entrainment of deep waters during winter cooling, and local stream runoff. The available supplies, the ambient seawater nitrate concentrations (C_∞) averaged over the duration of each mechanism, were compared with the estimated amount of nitrate utilized by kelp to determine the relative importance of each source mechanism to annual kelp nitrogen production.

Periods of strong upwelling were identified when surface water temperatures were below 13°C as per the methods of McPhee-Shaw et al. (2007). We considered strong upwelling only between March and May just as in McPhee-Shaw et al. (2007), but note that these months are not contiguous in time in our study, which included sampling in March–May 2005 and March–April 2006. We computed the amount of nitrate supplied to the forest during these periods and the amount taken up by the forest.

We quantified the role of internal waves in supporting net nitrate uptake using three approaches. We are unsure which of these three approaches best captures the contribution of internal waves, but together they provide bounds for the contribution of internal waves to nitrate delivery and use. First, we used the method of McPhee-Shaw et al. (2007) of identifying high internal wave activity as being those days during which diurnal temperature variance exceeded 0.70°C and used those periods to estimate nitrate supplied by internal waves and the amount of this nitrate acquired by kelp. Second, we estimated supply from internal waves as the difference between modeled hourly uptake based on hourly averaged nitrate concentrations and modeled hourly uptake based on concentrations calculated from median temperatures computed over the 1.5 d surrounding each hour of the study. Typical internal wave periods were less than 1.5 d. Uptake of nitrate from internal waves was calculated for each concentration time series and the difference in these values was taken as the amount of nitrogen production due to internal waves. A third approach was to estimate supply and uptake using nitrate concentrations calculated from temperatures measured only when flows through the kelp forest were moving onshore (e.g., Fig. 5). As in the second approach, the difference between results using concentrations measured at all times and those based on concentrations during onshore flow provided an

estimate of the supply and uptake of nitrate due to internal waves.

Buoyant plumes from terrestrial runoff could potentially concentrate nitrogen in surface waters where most kelp biomass occurs and where uptake kinetics are least light limited. We computed nitrogen input from local streams using data on stream discharge, nitrate concentration, and total dissolved nitrogen concentrations collected from nearby Arroyo Burro Creek and Mission Creek, which are located 1.5 km west and 3.8 km east of Mohawk Reef, respectively (Melack pers. comm.). Nitrate made up approximately 70% of the total dissolved nitrogen, and we assumed the constituents in the other 30% were taken up by *M. pyrifera* at the same rate as nitrate. We assumed stream inputs remained in nearshore waters for 24 h, where nearshore was considered to be within 700 m of shore, and within a 7-km alongshore region. We also assumed that stream inputs were well mixed in the upper 5 m of the water column. We believe that these rough length and time scale estimates are probably accurate within a factor of two based on sampling during storms (Brzezinski and Washburn unpubl.), on plume studies in the Southern California Bight (Grant et al. 2005), on the loading calculations of McPhee-Shaw et al., and on an approximation of the extent to which the kelp forests at Mohawk Reef and adjacent areas retard cross-shore nutrient dispersion. Loading is directly proportional to nearshore residence time and inversely proportional to the three length scales.

Utilization of nitrate supply—In addition to the uptake of nitrate associated with specific supply mechanisms, we estimated the percentage of total available nitrate taken up by the kelp in the forest over a year. The input of nitrate to the forest is the product of the concentration as a function of depth and time (C_∞) and the alongshore and cross-shore flows (Q_{along} and Q_{cross}, respectively) of water into the forest:

$$Q_{cross} = VHL$$
$$Q_{along} = UHW \qquad (13)$$
$$Q = Q_{cross} + Q_{along}$$

where V and U are the cross-shore and alongshore velocities inside the forest as a function of depth and time and L is the alongshore forest length, H is its depth, and W is its width. The amount of nitrate taken up by kelp is a product of the uptake per gram of kelp tissue and the average amount of kelp biomass per substrate area of the forest, as measured in a 40 m × 40 m portion of the forest by the SBCLTER. The fraction of the nitrate supply that is taken up by kelp is calculated as the time-average ratio of uptake by the forest to input to the forest.

Results

In this section we quantify the biological, physical, and chemical factors that affect nitrate uptake; we present results for our nitrate uptake model in the context of two sets of field measurements; we show the sensitivity of our model to each factor affecting uptake; and we apply our model over the entire kelp forest to evaluate the contribution of each nitrate source.

Oceanographic conditions affecting nitrate uptake—Temperature, wave period, wave height, and nitrate concentration varied during our study (Figs. 2–5). To separate the contribution of each supply mechanism to kelp nitrate uptake, we delineate periods with markedly different oceanic conditions using the depth-averaged water temperature, stratification quantified as buoyancy frequency, and wave data. A "cold" period containing each year's coldest surface water starts with a pulse of upwelling-favorable winds around the beginning of spring (2002–2007 http:// sbc.lternet.edu temperature data and regional upwelling index (UI) from www.pfeg.noaa.gov). In 2005, temperature dropped sharply below 13°C on 21 March (Fig. 2A). This water also had low stratification (<10 cycles h^{-1} Fig. 2B). A "stratified" period (12–19 cycles h^{-1}) occurred from 16 May to 02 September in 2005. The first portion of the stratified period (16 May–19 July) had cool temperatures averaging 14.6°C and strong upwelling index ($\overline{UI}=117$) while the remaining warm part averaged 17.3°C and had weak upwelling ($\overline{UI}=71$). A "warm destratifying" period occurred between 03 September and 28 November when water column properties transitioned from summer to winter conditions. Temperature declined to 15°C in the "cool unstratified" period, when stratification dropped to 8 cycles h^{-1}, and dominant wave period doubled from 6 to 12 s (Fig. 3A). The 2006 "cold" period, again indicated by temperatures dropping below 13°C and a spike in the regional upwelling index, began 06 March, 2 weeks earlier than in 2005. Based on 1985 through 2006 sea surface temperature (advanced very high resolution radiometer (AVHRR) and moderate resolution imaging spectroradiometer (MODIS)), our study occurred during a period with lower than average yet still typical temperatures and thus typical nitrate supplies. The 2005 and 2006 annual mean temperatures were the eighth and sixteenth coolest among the 22 yr of observation, the March through May temperatures were the tenth and eighth coolest, and the 2005 August through September temperature was seventh coolest.

Hydrodynamic conditions accompanying these series of regimes differed within and outside the kelp forest (Fig. 3B). Depth-averaged flow speeds at the inside station were 25% to 33% of those outside of the kelp forest until kelp biomass was reduced by large waves on 20 December 2005. After winter storms, current speeds inside the forest were 50% to 66% of the velocity outside the forest. Velocity at the outside station frequently exceeded the 4 to 6 cm s^{-1} threshold for mass-transport limitation; 74% of the time it exceeded 5 cm s^{-1}. Velocity at the inside station was above 5 cm s^{-1} 17% of the time before the large wave event and 53% subsequently.

Seawater nitrate concentration varied concurrently with shifts in hydrodynamics. It was highest during the cold periods (mean [NO$_3^-$] at the NAS 14.3 μmol L^{-1}), remained high during the stratified cool period (mean [NO$_3^-$] 4.5 μmol L^{-1}), and then declined to a mean concentration of 0.6 μmol L^{-1} during the warm stratified
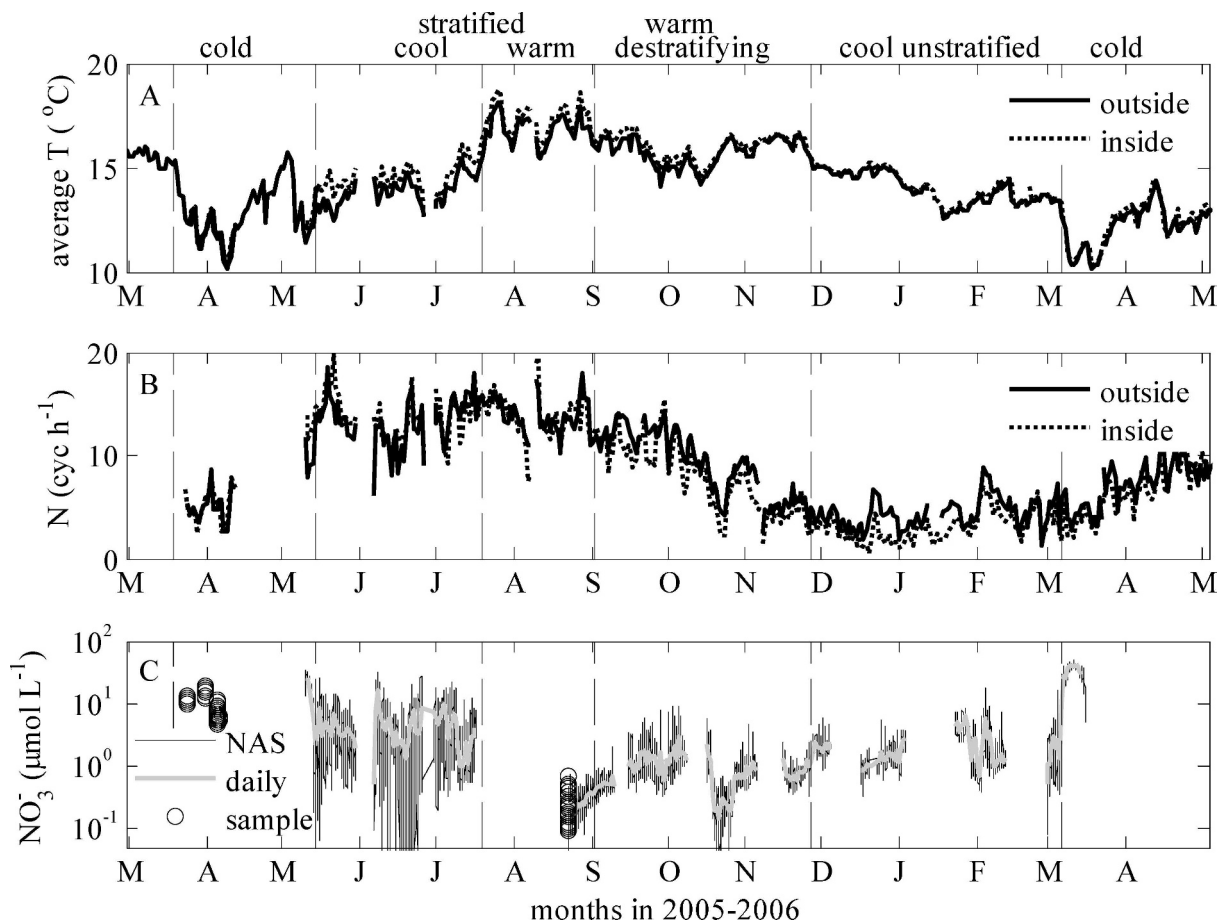
Fig. 2. (A) Daily depth-averaged temperature and (B) buoyancy frequency in cycles per hour inside and outside the kelp forest from March 2005 through April 2006 are used to demarcate periods of similar environmental conditions. (C) Shows nitrate concentrations at the outer edge of the kelp forest collected every 20 min by a nitrate autoanalyzing sensor (NAS), daily NAS averages (daily), and intermittent bottle sample data.

period (Fig. 2C). During the warm destratifying period mean nitrate concentration was 1.1 μmol L^{-1}, but concentrations less than 0.5 μmol L^{-1} occurred over multiple days in this period associated with "current reversals" that frequently occur in the Santa Barbara Channel (McPhee-Shaw et al. 2007). Nitrate concentrations during the cool unstratified (winter) period averaged 3.1 μmol L^{-1} and did not have multiday periods of very low concentration. Across depth, the concentration of nitrate was estimated by Eq. 1 to be an average of 6.9 times lower in the upper water column than at the bottom during the stratified period (summer) but only 1.4 times lower when stratification was at its annual minimum. Canopy nitrate concentration averaged 23% higher at the edge than in the interior during the stratified period and only 5% higher during the rest of the year.

Ambient nitrate concentrations were enormously variable in and around the kelp forest, particularly during the stratified period, when nitrate concentration varied by a factor of five to over two orders of magnitude within a single day (Fig. 2C). A positive relationship between low-frequency variability of temperature and nitrate concentration can be seen by comparing Fig. 2A and Fig. 2C,

while Fig. 4 shows that higher frequency nitrate concentration and temperature fluctuations were also coherent (Fig. 4B), particularly at the diurnal and semidiurnal frequencies in which most of the variations occurred (Fig. 4A). The diurnal and semidiurnal variations are associated with internal waves (Lerczak et al. 2003). An example of the effect of internal waves on the vertical temperature structure (and by proxy nitrate concentration) within the forest is given in Fig. 5. Cold waters penetrate from the lower portion of the forest twice each day; on reversal warm water from inshore infiltrates the forest. Temperature changes can be rapid (e.g., temperature increased by 2.5°C in less than an hour corresponding to a fivefold decrease in nitrate concentration).

Morphological characteristics of kelp affecting nitrate uptake—Seasonally, frond density increased from April through November, but density was reduced to near zero after the strong wave event in December 2005 (Fig. 6A). Surface area per mass (SAM^{-1}) for the canopy portions of growing canopy fronds was on average 5.2 times larger than SAM^{-1} in portions below the canopy (Fig. 6B). SAM^{-1} of canopy portions of fronds at the edge of the
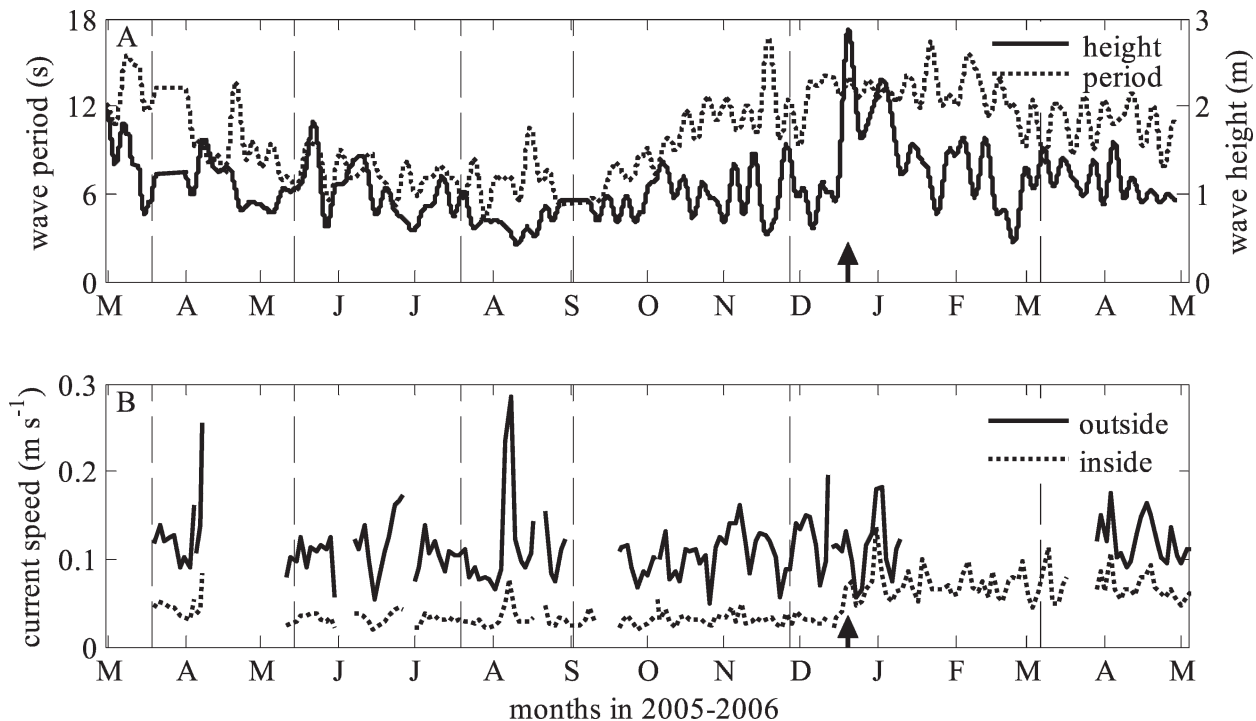
Fig. 3. (A) Dominant wave period and significant wave height measured at NOAA buoy 46216. (B) Depth-averaged velocity magnitude outside and inside the kelp forest. On 20 December 2005 (arrow) a large wave event removed most of the kelp biomass in the Mohawk kelp forest.
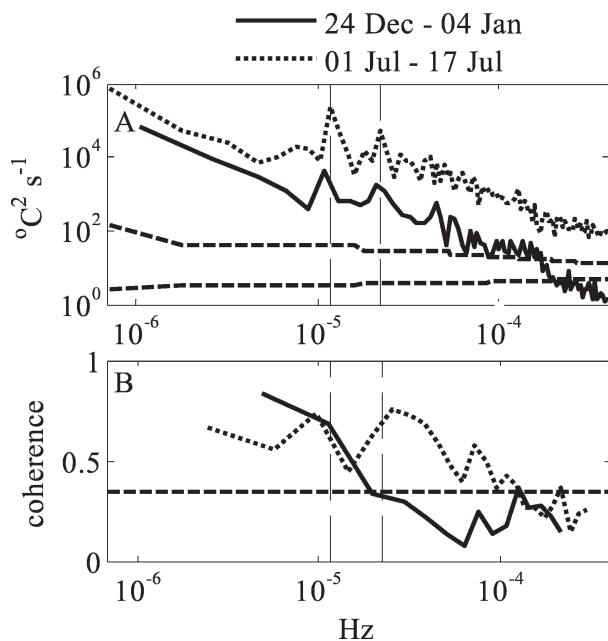

Fig. 4. (A) Temperature power spectra and (B) magnitude squared coherence between temperature and nitrate concentration during a period with energetic internal waves (01 to 17 July 2005) and weak internal waves (16 November to 05 December 2005). Vertical dashed lines mark diurnal and lunar semidiurnal (M2) periods. Horizontal dashed lines are 95% confidence bounds.

forest was twice that of fronds in the interior of the forest during the 2005 spring cold period, decreased to values similar to the interior by midsummer, and was less than fronds in the interior during the 2006 spring cold period.

Measured and modeled N *uptake rates*—Measured nitrogen acquisition in growing canopy fronds integrated over the water column (in units of mmol N (wet g)$^{-1}$ month^{-1}) varied by only a factor of six over the course of the year despite the two order of magnitude differences in ambient nitrate concentrations over the same time period (Fig. 7 vs. Fig. 2C). Nitrogen acquisition rates of growing canopy fronds declined continuously from a maximum of 0.32 mmol N g^{-1} month^{-1} in April, reaching 0.05 mmol N g^{-1} month^{-1} in November 2005, and then recovered to 0.1 mmol N g^{-1} month^{-1} in response to the increased nitrate concentrations during the first third of 2006, but not to the high levels observed in spring 2005. Measured specific rates at the edge of the forest were larger than in the interior by an average of 22%.

Rates of nitrogen acquisition per wet mass for fronds representative of the entire forest were generally lower and less variable than those based exclusively on growing canopy fronds. Nitrate uptake during the winter of 2005 was the highest since 2002 (the year SBCLTER began collecting such data), and the summer and fall 2005 uptake rates were the third and second lowest measured in the last 6 yr (data not shown). Maximum uptake rates of
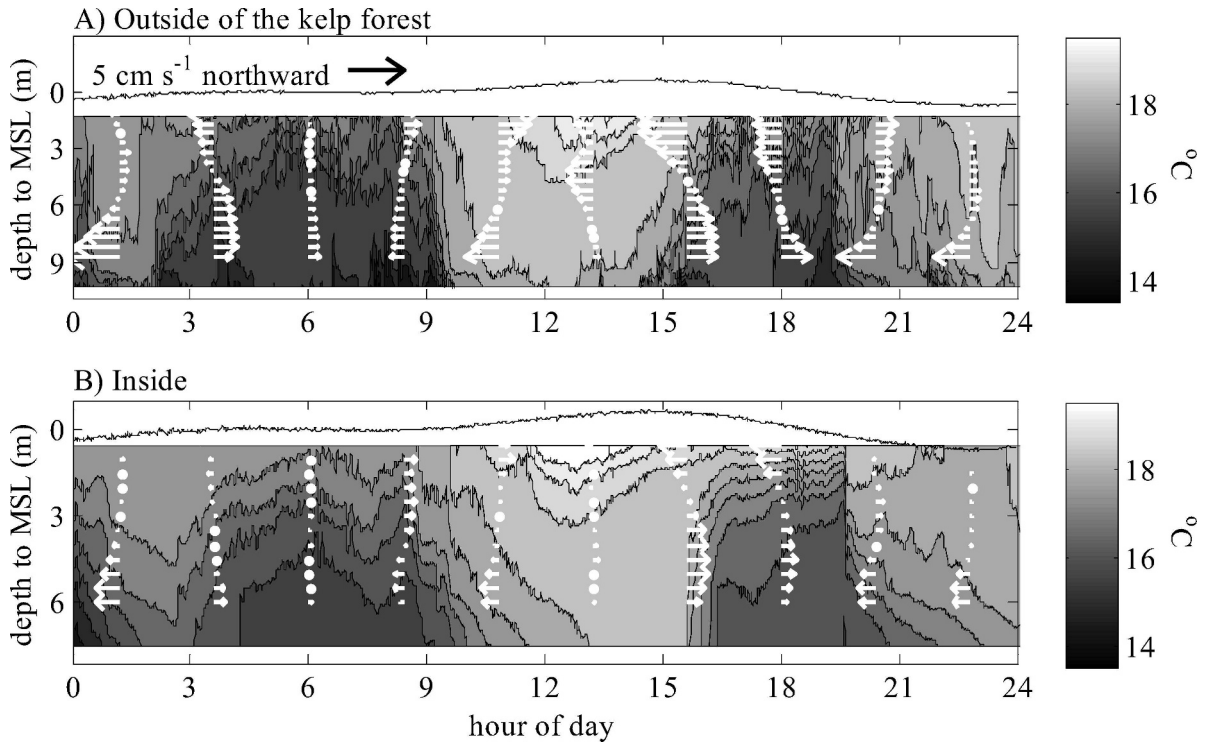
Fig. 5. Time series temperatures and cross-shore current velocities at the outside (A) and inside (B) stations on 26 August 2005 showing two internal waves propagating across the kelp forest. Contour intervals are 1°C. Onshore (northward) velocities are shown by white arrows pointing to the right. Tide levels are represented by black solid lines.
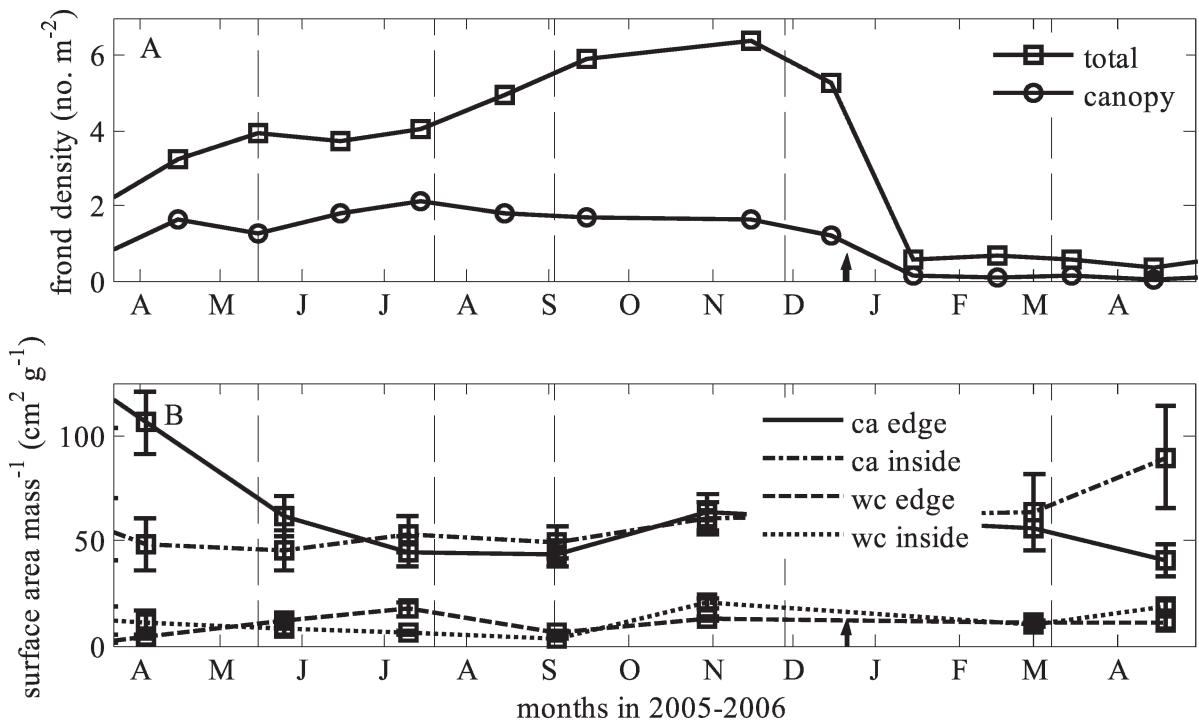

Fig. 6. (A) Monthly frond density (fronds per substrate area) at Mohawk Reef. (B) Surface area per wet mass in the canopy and the water column at the edge and in the interior of the Mohawk kelp forest.
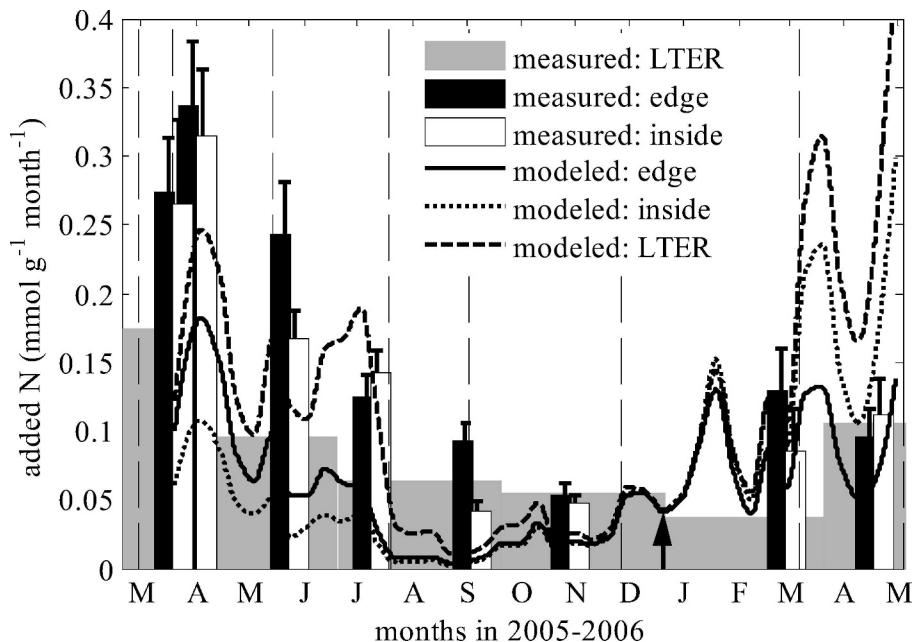
Fig. 7. Time series of measured acquisition and modeled uptake of nitrogen in mmol per wet g per month by growing canopy fronds at the edge and inside the Mohawk kelp forest, and of all fronds in a 40 m × 40 m area of the interior of the forest (LTER) for the period 21 March 2005 through 30 April 2006.

0.18 mmol N wet g^{-1} month^{-1} occurred during spring upwelling in 2005 and decreased fourfold by autumn (Fig. 7). Growing canopy fronds averaged 26% of the forest's total frond mass during the first 5 months of the study and dropped to 17% of the total mass after the 21 December 2005 storm.

Measured net nitrogen acquisition for growing canopy fronds was about double gross modeled uptake during the spring cold period in 2005, when the uptake kinetic parameters for nutrient-replete kelp were used (Fig. 7). Use of these kinetic parameters during spring cold and winter unstratified periods was supported by the analysis of blade tissue nitrate concentrations that showed relatively high levels of soluble nitrate, which is consistent with luxury uptake of a nonlimiting nutrient (2.5 ± 1.3 μmol (wet g)$^{-1}$ vs. 0.5 ± 0.5 μmol (wet g)$^{-1}$ at other times, Stewart unpubl. data). For this same period the model also overestimated nitrogen uptake rates for the LTER data set that contained both surface and subsurface fronds, although the overestimation was relatively small, averaging 37%. In the stratified and the warm destratifying periods, modeled uptake by both the growing canopy fronds (inside and edge) and by all the fronds (LTER) was much less than measured even when uptake parameters reflecting nutrient starvation were used in the model (Fig. 7). This deficit persisted until after the December 2005 storm, when modeled uptake again exceeded measured values.

Control of uptake by kinetics and mass transport—Model results indicate that nitrate flux was determined more by kinetics than by mass transfer. A plot of $RK_m/C_\infty V_{max}$ vs. $\beta K_m : V_{max}$ for the modeled nitrate fluxes grouped by periods of defined water conditions is shown in Fig. 8, with

selected constant values of $C_\infty : K_m$ plotted against $\beta K_m : V_{max}$ for reference. The asymptotes of the $C_\infty : K_m$ vs. $\beta K_m : V_{max}$ plots indicate exclusive control by kinetics (Sanford and Crawford 2000). Mean model results from all periods for $RK_m/C_\infty V_{max}$ are >90% of the maximum $RK_m/C_\infty V_{max}$ at their $C_\infty : K_m$ (Fig. 8). This finding indicates that uptake was controlled mainly by kinetics with only a small, but not negligible, influence of mass transfer.

The dominance of kinetics was most pronounced during the spring cold periods (Fig. 8) and for the few hours each day during the cool stratified period when internal waves brought high concentrations of nitrate into the forest (Fig. 2C). At these times $RK_m/C_\infty V_{max}$ was well above 90% of the maximum for its $C_\infty : K_m$. Equivalently at these times, blade surface concentrations (C_0) were well above 90% of C_∞. Mass transfer exerted its greatest influence on modeled nitrate flux in the unstratified winter and destratifying autumn periods. One might expect more mass transfer limitation during times of low nitrate concentration (July–September, Fig. 2C) than during the unstratified winter period because more mass transport was required due to kinetics allowing for flux at $C_\infty : \alpha$. However, the model predicted more mass-transport limitation during July through September than during the unstratified winter period because surface wave periods were shorter (Fig. 3A).

Distribution of nitrate uptake in the water column—The vertical distribution of modeled uptake in growing canopy fronds indicated relatively high rates of nitrate uptake in the canopy. Uptake by the canopy portions of growing canopy fronds was on average 88% of total modeled uptake over the entire time series (Fig. 9). This percentage
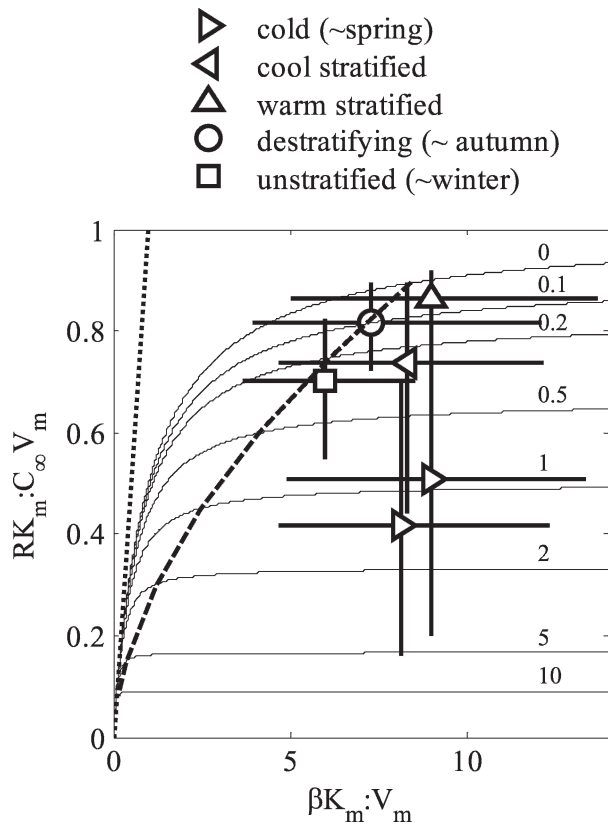
Fig. 8. Dimensionless uptake data graphed in a phase space based on dimensionless uptake vs. dimensionless mass transfer coefficients. Model results are grouped by seasonal conditions with bounds showing the range between the 5th and 95th percentile values. Solid curves are lines of constant $C_\infty : K_m$. Kinetic limitation dominates to the right of the dashed line, which connects points of 90% of the asymptotic values of the $C_\infty : K_m$ lines. R equals βC_∞ along the 1 to 1 line (dotted line) and specifies where there is no kinetic limitation.

decreased for a brief period in early summer when stratification was high and new fronds proliferated below the canopy. During late summer and autumn, the canopy comprised 64% of the biomass of growing canopy fronds. However, despite higher nitrate concentrations at depth during late summer and autumn, mean percentage canopy uptake of growing canopy fronds was higher than 64%. This anomalous situation occurred because biomass at depth was less efficient at taking up nitrate due to lower surface area per mass (Fig. 6A) and lower $V_{\max}$ due to reduced irradiance with depth.

Total nitrate supply to the forest and the forest's utilization efficiency—We computed the percentage of available nitrate taken up by the kelp forest, which involved computing nitrate supplies coming from both alongshore and cross-shore directions (Eq. 13). Vertical shear in the alongshore direction was small ($U(t, z) \cong \overline{U}(t)$), and depth-average flow in the cross-shore direction was small ($\overline{V}(t) \cong 0$), so we refer to the alongshore flow as barotropic and the cross-shore flow as baroclinic. Because the nitrate-rich water originates offshore, we expected that the vast

majority of the nitrate input to the forest would be from cross-shore baroclinic exchange. However, only 55% of nitrate input to the forest was from cross-shore baroclinic exchange, while the remaining portion was from along-shore flow, implying that waters went through adjacent kelp forests and other inshore areas for an extended period of time without losing a significant amount of nitrate. Comparing the alongshore and cross-shore supplies with modeled uptake and measured net acquisition, we show that the kelp bed used only up to 5% of the nitrate supplied to the forest (Fig. 10). This low percentage of utilization supports our use of the same nitrate-to-temperature relationship at the edge and interior of the forest for modeling nitrate concentrations. As further validation, our measurements of nitrate and temperature at the edge and interior of the forest for 2 weeks in fall 2006 yielded indistinguishable nitrate-to-temperature relationships de-spite kelp density and thus nitrate uptake being higher than during our 13-month experiment (10 fronds m^{-2} vs. a maximum of 6.3 fronds m^{-2} in Fig. 6A) and nitrate concentration being low (median 0.3 μmol L^{-1}).

Sources of nitrate in support of kelp growth—Most of the modeled uptake occurred during times when nitrate supply derived from upwelling, that is, during the 2005 and 2006 cold periods and the stratified cool period (Table 1). Winter cooling increased concentrations during the cool unstratified period, but there was not much kelp in the forest during this period, so consequently little nitrate uptake occurred. Modeled uptake from local runoff was negligible because it was a small portion of overall supply and those supplies occurred both when the kelp forest was sparse and when other nitrate sources were in large supply (Table 2). In contrast, internal waves, which also accounted for a small portion of overall nitrate supply based on all three calculation methods, made a much larger contribu-tion to kelp nitrogen demand than runoff, because they were most intense during the period in which there was the least amount of nitrate available from other sources and when the kelp biomass in the forest was high (Table 2). The mechanisms for bringing upwelled water inshore to this part of the Santa Barbara Channel during stratified periods are not fully understood, but this data set links internal tides to its delivery.

Discussion

Mass transport vs. kinetic limitation—Our dimensionless analysis indicated that nitrate uptake by kelp at Mohawk Reef was largely controlled by concentration-dependent kinetics and to a lesser extent by mass transfer (Fig. 8). We expected that mass transport would vary within the kelp forest as a result of spatial differences in current speeds and waves (Fig. 3) and that this difference might explain our observation that uptake was higher at the edge than in the interior. However, replacing inside velocities with the higher outside velocities increased modeled uptake by less than 1%. This modeled increase was small because while steady-current fluxes (Eq. 8) were higher because of the thinner viscous sublayer under the faster currents, the flux
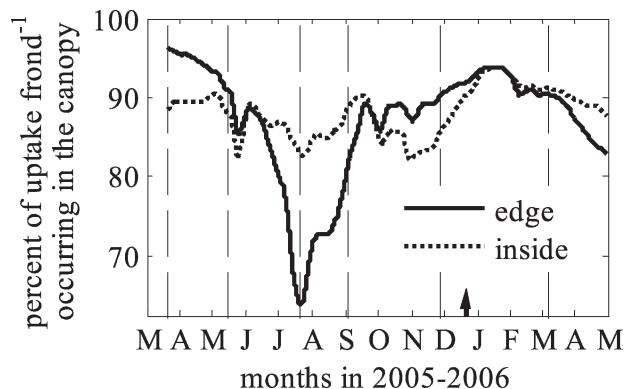
Fig. 9. Time series of the percentage modeled uptake that occurs in the surface canopy for actively growing fronds that reached the sea surface.
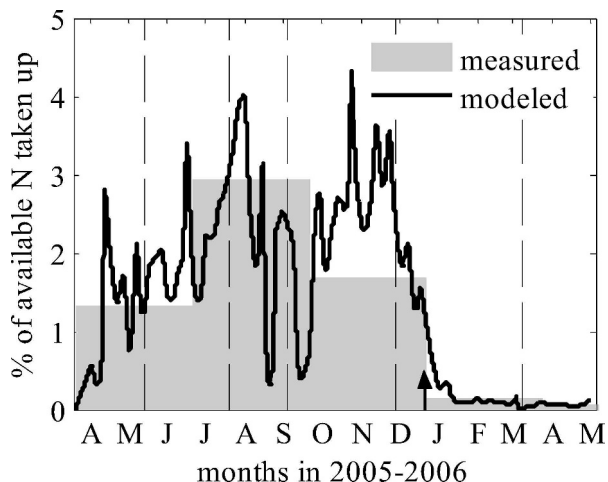

Fig. 10. Percentage of nitrate delivered to the forest that is taken up by giant kelp based on modeled uptake and measured acquisition by all fronds in the interior of the kelp forest.

from boundary layer stripping (Eq. 10) was reduced because the linear steady-current diffusive boundary layer profile developed more quickly when the boundary layer was thin. Essentially, waves facilitated mass transfer more than currents, and our model predicted that waves were slightly more efficient at mass transport when currents were smaller, as was the case at the inside station. Thus, factors other than currents, such as light availability, must account for uptake differences between the edge and the interior fronds.

Utilization efficiency—Residence time of water within the kelp forest, along with kelp density and uptake characteristics, determines the use of ambient nitrogen. For all but 1 month of the study, the modeled utilized portion of the nitrate passing through this kelp forest was less than 5% (Fig. 10). This suggests that the Mohawk kelp forest was not large enough during our study for uptake by upstream fronds to dramatically limit the nitrate exposure of interior fronds. Maximum use occurred at the end of October during a current reversal in what has been characterized as "flood west" conditions by Harms and Winant (1998). Surface currents over the entire channel (www.oceancurrentmaps.net) were westward at this time as opposed to their more common cyclonic orientation. They brought cool, but nutrient-depleted water across the Santa Barbara Channel where our study site was located.

The percentage of available nitrogen utilized by giant kelp is among other things proportional to the residence time of seawater nitrate in the forest, which we can relate to the residence time of seawater. Seawater residence time, which we calculated from the flow into the forest and the forest volume (LWH:Q), averaged 1.1 h. Exchange through Mohawk Reef was roughly equivalent between alongshore (45%) and cross-shore flows (55%). In contrast, residence time was longer in the much larger Point Loma kelp forest, where exchange is dominated by cross-shore baroclinic currents (Jackson and Winant 1983). Alongshore flow was not important to exchange in the Point Loma forest, since alongshore currents flushed the forest only once a week and the time scale for nitrate uptake was 4 h.

No nitrate depletion was observed (North et al. 1986), an observation that attests to the importance of cross-shore nitrate delivery. Thus, our results illustrate a distinction between the processes affecting the function of large and moderate-sized kelp forests.

Sources of nitrate in support of kelp growth—Similar to McPhee-Shaw et al. (2007), we found that upwelling supplied the vast majority of the nitrate to the water in our kelp forest. Using concentration at the NAS mooring as a proxy for nitrate supply, we infer 68% of the seawater nitrate supplied during the 13-month study occurred during the two early spring cold periods dominated by upwelling and 13% occurred during the stratified period influenced by upwelling-favorable winds. Perhaps a more appropriate method of characterizing the nitrate supply to the kelp forest is to define it as the temporal change as a function of depth in the product of kelp surface area and seawater nitrate concentration. By this accounting of dynamic changes in forest biomass and biomass distribution, we found that 58% of the seawater nitrate exposure occurred during the two early spring cold periods dominated by upwelling and 20% occurred during the stratified period influenced by upwelling. The large nitrate exposure from the upwelling-influenced periods supported 50% of the measured net nitrogen acquisition by the forest during the study period (Table 1). Modeled uptake within the LTER transect area exceeded net acquisition during strong upwelling, suggesting that fronds replete with nitrogen reduce their uptake characteristics (V_{max}) more than we simulated in the model, although there may also be other idealizations or factors not considered in the model that influenced the comparison. Other sources supplied significant amounts of the nitrogen taken up by the kelp during nonupwelling periods (Fig. 7, Table 1).

The role of internal waves in nitrate supply is difficult to quantify because internal wave activity is superposed upon upwelling and other processes that effect nitrate concentrations in nearshore regions. These processes, as well as

Table 1. Uptake by period: Modeled uptake and measured nitrogen acquisition per area of ocean bottom calculated for the six time periods with distinct oceanic conditions. Values are based on data collected by SBCLTER in a 40 m $\times$ 40 m area in the interior of the kelp forest. Nitrate exposure for each time period is the product of the mean concentration of nitrate in seawater at each depth and the surface area of all fronds at each depth divided by the frond's total surface area.

Period	Date	Modeled gross uptake (μmol m^{-2})	Measured net acquisition (μmol m^{-2})	Exposure (μmol)	No. of days
2005 cold period with upwelling	21 Mar 05–16 May 05	749	469	9.7	55
Stratified cool period with upwelling	16 May 05–20 Jul 05	1,041	590	2.8	66
Stratified warm period without upwelling	20 Jul 05–03 Sep 05	135	411	0.4	45
Warm destratifying	03 Sep 05–28 Nov 05	397	554	0.9	86
Cool unstratified	28 Nov 05–06 Mar 06	298	186	2.2	100
2006 cold period with upwelling	06 Mar 06–30 Apr 06	145	98	16.1	54
Total		2,765	2,308	3.0	406

ones that either bring nutrient-poor water or cause a drawdown of nitrate in the upper water column, should likely be considered as the main processes affecting supply. We propose that internal waves, with their twice daily upwelling and ensuing 10- to 100-fold increases in ambient concentrations in the kelp forest, augment the overall nitrate supply. Internal waves were strongest in the late spring and early summer, overlapping with the first half of the period with annual lows in seawater nitrate concentration and annual highs in kelp abundance. Consequently, internal waves played a disproportionately large role in sustaining the kelp relative to their contribution to the total nitrogen supply (Table 2). Our analyses indicated that nitrate delivered by internal waves accounted for up to 27% of the nitrogen demand by kelp during summer and fall (384 + 35 μmol m^{-2} from the second row of Table 2 vs. 1041 + 135 + 397 μmol m^{-2} from the first column of Table 1). The extent of the augmentation of nitrate supply by internal waves in different years will depend upon the length of the stratified period (*see* www.opl.ucsb.edu), the depth of the pycnocline in relation to the nutricline, and the forcing processes that determine the amplitude of the internal waves and their penetration into nearshore waters.

The importance of freshwater supply of nutrients must be addressed in the context of variability of other supply mechanisms. During our study, total freshwater inflow was small and all of the runoff events occurred during winter and spring periods when seawater nitrate concentrations were high and kelp abundances were low. Nitrogen inputs from local streams may be more important in other years. Our 13-month study spanned the 16th lowest amount of rainfall in the last 57 yr among similar time periods (21 March through 30 April the following year) based on National Climate Data Center rainfall data. Also, our study did not occur during an El Niño year, which in southern California is usually accompanied by warm nutrient-poor ocean waters and high rainfall. Furthermore, rainfall and resulting stream discharge did not occur during the nutrient-poor period, but large storms between July and October have occurred in other years (4 of the last 57). Thus year to year variations in the timing of storm runoff will determine the importance of freshwaters as a nutrient source.

From mid-July through the end of November, modeled nitrogen uptake to all fronds and to only that of growing canopy fronds was much less than the achieved nitrogen acquisition. We do not believe this discrepancy is due to underestimating $V_{max} : K_m$ in the first-order kinetics portion of the model. Although a wide range of ecotypic uptake characteristics has been observed for *M. pyrifera* in southern California (Kopczak et al. 1991), measurements of *M. pyrifera* uptake plasticity indicate that the increases

Table 2. Acquisition by kelp of nitrate supplied by internal waves estimated using three different methods and by stream runoff. Additional nitrate concentration due to each mechanism and modeled and measured rates of nitrogen acquisition from each mechanism were calculated for the entire 13-month study period, the cool stratified nitrate-rich period influenced by upwelling, and the warm nitrate-poor period (20 Jul–28 Nov 2005).

Source	[NO$_3$] (μmol)	Modeled nitrogen acquisition by giant kelp (μmol m^{-2})		
		Entire study period	Stratified period with upwelling	Warm, low nitrate period
Local stream runoff	0.11	66	<1	<1
Internal waves from temperature variance	0.27	424	384	35
Internal waves from 1.5-d median	0.31	224	155	51
Internal waves from onshore flow	0.25	151	81	35
Mean internal wave influence	0.27	266	207	40

in uptake capabilities required to meet our observed nitrogen acquisition are unrealistic (Kopczak 1994). Thus, we are led to believe that there are other sources of nitrogen available to the kelp in summer and fall. Our analysis suggests that these other sources must supply over half of the nitrogen demand by kelp from 20 July through 28 November 2005 (Table 1: measured vs. modeled columns). Gerard (1982b) and Hepburn and Hurd (2005) have suggested that epibionts may provide enough nitrogen in the form of excreted ammonia to support kelp growth. Kelp blades at our site were encrusted with bryozoans of the genus *Membranipora* during late summer in 2005 (K. Arkema, pers. comm.). Using a maximum percentage surface area of *Macrocystis* fronds covered by epibionts of 7% (Hepburn and Hurd 2005) and an excretion rate of 6 nmol m^{-2} s^{-1} (Hepburn pers. comm. 2007), we estimate that the excretion of ammonia by *Membranipora* averaged 0.12 mmol g^{-1} $month^{-1}$ for fronds in the SBCLTER transect area during the warm stratified period and 0.14 mmol g^{-1} $month^{-1}$ from 09 September 2005 through 28 November 2005. Both of these values are large enough to account for the discrepancies between measured and modeled uptake (Fig. 7). Although we do not know what proportion of the excreted ammonia might have been taken up by kelp, the potentially high excretion values and the low concentration of nitrate provide support for the role of recycling, particularly by epibionts, in *M. pyrifera* nitrogen supply.

This study has not only shown the percentage contribution of various physical processes in supplying nitrate to a kelp forest, it has addressed the role of hydrodynamics within the forest and surrounding the kelp blades on nutrient acquisition. In moderately sized kelp forests, the residence time of water is short because of supplies from both alongshore and cross-shore directions, so ambient nitrate concentrations are not drawn down by upstream kelp. Nitrate concentrations are high enough in all seasons that nitrate uptake is primarily governed by kinetics as opposed to mass transfer. We have extended the recent analyses done by McPhee-Shaw et al. (2007) of nutrient supply from various oceanographic processes to kelp forests in this region by going from analyses of nitrate concentration at a forest's edge to a description of concentration across a kelp forest and of a forest's ability to take advantage of nitrate supplies because of the location and abundance of frond surface area. We have created a budget that contrasts modeled uptake rates of nitrate with measured uptake of nitrogen. With this budget, we determined that remineralized or recycled nutrients are the source of ~50% of the inorganic nitrogen taken up by kelp from midsummer through midfall 2005. In larger beds with their greater flow reduction, upstream kelp may affect nitrate supply, mass transfer limitation may play a larger role, and the number of epibionts that attach to fronds may be lower, as well as the flux of phytoplankton on which they feed. In these larger beds, either fronds would become more nitrogen stressed or other mechanisms of recycling may be operative. Overall, we have quantified for the first time the contribution of both physical oceanographic and biological processes to supply and uptake of nitrogen by a kelp forest. With these insights, we are positioned for a greater understanding of the implications of changing oceanographic conditions on kelp forests of various sizes.

References

BECKENBACH, E., AND L. WASHBURN. 2004. Low frequency waves in the Santa Barbara Channel observed by high-frequency radar. J. Geophys. Res. Ocean. **109:** C02010, doi: 10.1029/2003JC001999.

CLENDENNING, K. 1971. Photosynthesis and general development p. 257–263. *In* W. J. North [ed.], The biology of giant kelp beds (*Macrocystis*) in California. Hedwigia, Verlag Von J. Cramer.

GAYLORD, B., AND OTHERS. 2007. Spatial patterns of flow and their modification within and around a giant kelp forest. Limnol. Oceanogr. **52:** 1838–1852.

GERARD, V. A. 1982a. Growth and utilization of internal nitrogen reserves by the giant kelp *Macrocystis pyrifera* in a low-nitrogen environment. Mar. Biol. **66:** 27–35.

———. 1982b. In situ rates of nitrate uptake by giant kelp, *Macrocystis pyrifera* (L.) C. Agardh: Tissue differences, environmental effects, and predictions of nitrogen-limited growth. J. Exp. Mar. Biol. Ecol. **62:** 211–224.

———. 1982c. In situ water motion and nutrient uptake by the giant kelp *Macrocystis pyrifera*. Mar. Biol. **69:** 51–54.

GRAHAM, M. H., J. A. VASQUEZ, AND A. H. BUSHMAN. 2007. Global ecology of the giant kelp *Macrocystis*: From ecotypes to ecosystems. Oceanogr. Mar. Biol. Annu. Rev. **45:** 39–88.

GRANT, S. B., J. H. KIM, B. H. JONES, S. A. JENKINS, J. WASYL, AND C. CUDABACK. 2005. Surf zone entrainment, along-shore transport, and human health implications of pollution from tidal outlets. J. Geophys. Res. **110:** 1–20.

HARMS, S., AND C. D. WINANT. 1998. Characteristic patterns of the circulation in the Santa Barbara Channel. J. Geophys. Res. **103C2:** 3041–3065.

HEPBURN, C. D., AND C. L. HURD. 2005. Conditional mutualism between the giant kelp *Macrocystis pyrifera* and colonial epifauna. Mar. Ecol. Prog. Ser. **302:** 37–48.

HURD, C. L., P. J. HARRISON, AND L. D. DRUEHL. 1996. Effect of seawater velocity on inorganic nitrogen uptake by morphologically distinct forms of *Macrocystis integrifola* from wave-sheltered and exposed sites. Mar. Biol. **126:** 205–214.

JACKSON, G. A. 1977. Nutrients and production of giant kelp, *Macrocystis pyrifera,* off southern California. Limnol. Oceanogr. **22:** 979–995.

———. 1984. Internal wave attenuation by coastal kelp stands. J. Phys. Oceanogr. **14:** 1300–1306.

———. 1998. Currents in the high drag environment of a coastal kelp stand off California. Cont. Shelf Res. **17:** 1913–1928.

———, AND C. D. WINANT. 1983. Effect of a kelp forest on coastal currents. Cont. Shelf Res. **2:** 75–80.

KAMACHI, K., Y. AMEMIYA, N. OGURA, AND H. NAKAGAWA. 1987. Immuno-gold localization of nitrate reductase in spinach (*Spinacia oleracea*) leaves. Plant Cell Physiol. **28:** 333–338.

KOPCZAK, C. D. 1994. Variability of nitrate uptake capacity in *Macrocystis pyrifera* (Laminariales, Phaeophyta) with nitrate and light availability. J. Phycol. **30:** 573–580.

———, R. C. ZIMMERMAN, AND J. N. KREMER. 1991. Variation in nitrogen physiology and growth among geographically isolated populations of the giant kelp, *Macrocystis pyrifera* (Phaeophyta). J. Phycol. **27:** 149–158.

LERCZAK, J. A., C. D. WINANT, AND M. C. HENDERSHOTT. 2003. Observations of the semidiurnal internal tide on the southern California slope and shelf. J. Geophys. Res. Oceanogr. **108 C3:** 3068, doi:10.1029/2001JC001128.

LI, Y. H., AND S. GREGORY. 1974. Diffusion of ions in sea water and in deep-sea sediments. Geochim. Cosmochim. Acta **38:** 703–714.

MANN, K. 1973. Seaweeds—their productivity and strategy for growth. Science **182:** 975–981.

McPHEE-SHAW, E. E., D. A. SIEGEL, L. WASHBURN, M. A. BRZEZINSKI, J. L. JONES, A. LEYDECKER, AND J. MELACK. 2007. Mechanisms for nutrient delivery to the inner shelf: Observations from the Santa Barbara Channel. Limnol. Oceanogr. **52:** 1748–1766.

MIFLIN, B. J. 1974. The location of nitrite reductase and other enzymes related to amino acid biosynthesis in the plastids of root and leaves. Plant Physiol. **54:** 550–555.

NORTH, W. J., G. A. JACKSON, AND S. L. MANLEY. 1986. *Macrocystis* and its environment, knowns and unknowns. Aquat. Bot. **26:** 9–26.

RASSWEILER, A., K. K. ARKEMA, D. C. REED, R. C. ZIMMERMAN, AND M. A. BRZEZINSKI. In press. Net primary production, growth and standing crop of *Macrocystis pyrifera* in Southern California. Ecology.

SANFORD, L. P., AND S. M. CRAWFORD. 2000. Mass transfer versus kinetic control of uptake across solid-water boundaries. Limnol. Oceanogr. **45:** 1180–1186.

STEVENS, C. L., AND C. L. HURD. 1997. Boundary-layers around bladed aquatic macrophytes. Hydrobiologia **346:** 119–128.

————, ————, AND P. E. ISACHSEN. 2003. Modelling of diffusion boundary-layers in subtidal macroalgal canopies: The response to waves and currents. Aquat. Sci. **65:** 81–91.

WHEELER, P. A., AND W. J. NORTH. 1981. Nitrogen supply, tissue composition and frond growth rates for *Macrocystis pyrifera* off the coast of southern California. Mar. Biol. **64:** 59–69.

WHEELER, W. N. 1980. Effect of boundary layer transport on the fixation of carbon by the giant kelp *Macrocystis pyrifera*. Mar. Biol. **56:** 103–110.

ZIMMERMAN, R. C., AND J. N. KREMER. 1984. Episodic nutrient supply to a kelp forest ecosystem in Southern California. J. Mar. Res. **42:** 605–632.

————, AND ————. 1986. In situ growth and chemical composition of the giant kelp, *Macrocystis pyrifera*: Response to temporal changes in ambient nutrient availability. Mar. Ecol. Prog. Ser. **27:** 277–285.

————, AND D. L. ROBERTSON. 1985. Effects of El Nino on local hydrography and growth of the giant kelp, *Macrocystis pyrifera,* at Santa Catalina Island, California. Limnol. Oceanogr. **30:** 1298–1302.